INORGANIC CHEMISTRY
FRONTIERS

RESEARCH ARTICLE

View Article Online
View Journal | View Issue

Cite this: *Inorg. Chem. Front.*, 2025, **12**, 4494

A DNA aptamer for trivalent lanthanide ions with low nanomolar affinity†

Jin Wang,[a,b] Xin Wang,[b,c] Xuesong Li,[b,d] Xiangmei Li,[a] Hongtao Lei[a] and Juewen Liu*[b]

Received 9th February 2025,
Accepted 4th April 2025

DOI: 10.1039/d5qi00391a

rsc.li/frontiers-inorganic

Lanthanides are extremely important for a variety of technological applications. In this work, DNA aptamers were selected using the library-immobilization method (capture-SELEX) with Tb^{3+} and Ce^{3+} as target metal ions. The Tb^{3+} selection yielded a new sequence named Tb-1 that has a K_d of 26.9 nM for La^{3+}, 3.9 nM for Tb^{3+}, and 2.3 nM for Lu^{3+} as determined by a DNA strand displacement assay. Non-lanthanide metal ions did not induce a fluorescence enhancement. Therefore, it is a general lanthanide binding aptamer. Another aptamer Tb-4 (K_d 290 nM) has some sequence similarity to a previously reported aptamer selected using Gd^{3+} (K_d 1.5 μM), as determined by a thioflavin T fluorescence assay. Compared to a previously reported aptamer named Sc-1, Tb-1 has faster exchange with EDTA for lanthanide binding, suggesting that Tb-1 is an outer-sphere ligand. By comparing different aptamers, we have gained fundamental insights into aptamer binding to lanthanide ions. Finally, using the strand displacement reaction, a detection limit of 0.5 nM Tb^{3+} was achieved in Lake Ontario water.

Introduction

Lanthanide ions comprise a group of 15 metal ions within the *f*-block of the periodic table. They are extremely important in modern technologies.[1,2] With rich *f*-orbitals, lanthanide ions have unique optical and magnetic properties, allowing them to be used in magnetic imaging contrast agents, permanent magnets and upconverting nanoparticles.[3,4] Yet, they all have similar chemical properties since electrons in the *f*-orbitals are shielded and do not usually participate in chemical bonding. Lanthanides are further categorized based on their atomic numbers to be light (from lanthanum to europium) and heavy (from gadolinium to lutetium).[5]

Lanthanide ions can be accurately measured by inductively coupled plasma optical emission spectroscopy (ICP-OES),[6–8] and ICP mass spectrometry (ICP-MS).[9,10] However, these techniques require expensive instruments and can hardly be implemented for on-site and real-time detection. Many chemical probes have been developed for the detection of lanthanide ions,[11,12] but most are less sensitive or selective. Lanthanide binding proteins have also been discovered with high binding affinity, although using them for detecting lanthanides could be challenging due to cost, stability and signal transduction considerations.[13–15]

DNA is composed of four types of nucleosides attached to a phosphate backbone, and both nucleobases and phosphate can bind to lanthanide ions.[16–18] Attempts have been made to use DNA to detect lanthanides. Using a method called *in vitro* selection, our lab previously isolated five DNAzymes that can cleave an RNA substrate in the presence of trivalent lanthanide ions.[2,19–22] These DNAzymes have different activity trends cross the lanthanide series, and in general they do not respond to non-lanthanide ions. Other groups also used lanthanide ions to catalyze reactions such as DNA cleavage.[23] DNAzymes catalyze chemical reactions and they may not directly bind to lanthanides. It is important to isolate aptamers[24–27] for lanthanide ions to achieve advanced applications such as separation, enrichment and detection.

A DNA aptamer named Ln-aptamer for Gd^{3+} was reported by Edogun and coworkers. To avoid confusion, in this work, we renamed it Gd-1.[28] Their goal was to use this aptamer for the detection of free Gd^{3+} ions to ensure the safety of gadolinium-based contrast agents. The authors speculated that this aptamer can bind to all the lanthanide ions but they only measured binding using Gd^{3+}. Our lab recently used the capture-SELEX method to isolate aptamers for Sc^{3+}. Interestingly, this Sc^{3+} aptamer named Sc-1 can bind to all the trivalent lanthanide ions, and binding is stronger for heavier

[a]*Guangdong Provincial Key Laboratory of Food Quality and Safety, College of Food Science, South China Agricultural University, Guangzhou 510642, China*
[b]*Department of Chemistry, Waterloo Institute for Nanotechnology, University of Waterloo, Waterloo, Ontario N2L 3G1, Canada. E-mail: liujw@uwaterloo.ca*
[c]*Beijing Laboratory for Food Quality and Safety, College of Food Science and Nutritional Engineering, China Agricultural University, Beijing 100083, China*
[d]*School of the Environment and Safety Engineering, Jiangsu University, Zhenjiang 212013, China*

†Electronic supplementary information (ESI) available. See DOI: https://doi.org/10.1039/d5qi00391a

lanthanide ions. Based on the binding affinities and kinetics of Sc-1, rare earth elements were categorized into three groups.[29]

Since we already have an aptamer that binds to heavier lanthanides more strongly, in this work, we selected aptamers using terbium (Tb^{3+}) and cerium (Ce^{3+}). Tb is in the middle of the lanthanide series and is best known for its optical property with strong green emissions. Ce is a light lanthanide and it is often used in catalysis. In the end, we discovered an ultrahigh affinity aptamer that can bind to all the lanthanides with a similar affinity, so that the lanthanides can be detected as a group.

Materials and methods

Systematic evolution of ligands by the exponential enrichment (SELEX)

The SELEX experiments were conducted using the library immobilization following established procedures.[30,31] The SELEX buffer contain 10 mM MES, pH 6.0, 100 mM NaCl, 2 mM $MgCl_2$. $TbCl_3$ hexahydrate and $CeCl_3$ heptahydrate were dissolved in Milli-Q water at 100 mM. Then, they were diluted with SELEX buffer. The Tb^{3+} concentration was 10 μM for rounds 1 to round 7, 2 μM for rounds 8 and 9, 200 nM for round 10, and 100 nM for rounds 11 and 12. For the Ce^{3+} selection, the Ce^{3+} concentration was 10 μM for rounds 1 to 14 and 2 μM for rounds 15 and 16. The PCR products from the last rounds were deep sequenced at the facility in McMaster University.

Thioflavin T (ThT) fluorescence-based binding assays

ThT fluorescence assays were conducted using a variant eclipse fluorescence spectrophotometer. A mixture containing 2.5 μL aptamer (100 μM), 5 μL ThT (100 μM) and 492.5 μL SELEX buffer was prepared. The mixture was then transferred to a quartz cuvette followed by titration with Tb^{3+} or other metal ions. The fluorescence intensity at 490 nm was recorded for analysis. The dissociation constant (K_d) was determined by fitting the equation: $F = F_0 + AK_d/(K_d + x)$, where x denotes the concentration of the metal ion, and A denotes the maximal fluorescence variation upon full binding.[30,32]

Fluorescent DNA strand-displacement sensor

The strand displacement sensor was tested in a 96-well microplate using a microplate reader (Tecan Spark F200Pro). 1 μL of FAM-labeled Tb-1 aptamer (100 μM) and 2 μL of quencher-labeled DNA (100 μM, Table S1†) were mixed in 97 μL SELEX buffer. This mixture was annealed at 85 °C and gradually cooled to room temperature, followed by incubation at 4 °C for 30 min and storage at −20 °C for an additional 30 min. The background fluorescence of the sensor was stabilized and recorded for 5 min before adding 2 μL Tb^{3+} or other metal ions. The kinetics of fluorescence signal change were then monitored for 10 min (Ex: 485 nm, Em: 520 nm). Each experiment was performed in triplicate.

Results and discussion

Selection of aptamers for Tb^{3+}

The capture-SELEX method was employed for aptamer selection,[29–31] which started by the immobilization of a DNA library containing 30 random nucleotides *via* hybridization to a biotinylated capture strand (15 base pairs) bound to streptavidin agarose beads. After washing away unbound DNA, the immobilized library was then incubated with Tb^{3+}. Some aptamers might be released from the capture strand upon binding to Tb^{3+}, and the released DNA strands were amplified by PCR. We monitored the progress of the selection using real-time PCR by comparing the released DNA concentration eluted by buffer elution and by the same buffer containing Tb^{3+}. The Tb^{3+} concentration was gradually decreased from 10 μM to 100 nM during the 12 rounds of selection. In the first 5 rounds, it appeared that more DNA was released by the buffer (Fig. S1†), suggesting that Tb^{3+} might have inhibited PCR. This phenomenon was also observed in our previous Sc^{3+} selection.[29] Since round 7, the Tb^{3+} eluted DNA caught up and the PCR cycle difference reached 5, indicating the enrichment of Tb^{3+} binding aptamers. The PCR product of round 12 was deep sequenced.

We ranked the sequences and the most abundant sequence named Tb-1 has only 218 copies (~1% of the sequence obtained), whereas the rest of the sequences were all below 100 copies. Therefore, there were still a lot of diversity in the library, suggesting a large sequence variety of Tb^{3+} aptamers. To have an overall understanding, the top 10 sequences were aligned. We observed one family and some ungrouped sequences as shown in Fig. 1A. This family comprises 7 sequences, featuring conserved regions marked in red, and complementary base pairs highlighted in yellow. The first sequence in this family is named Tb-4. Tb-4 has a very clear secondary structure containing a large hairpin region and a conserved loop (Fig. 1C). Binding of Tb^{3+} likely takes place in the loop region. We also studied Tb-1, since it is the most abundant sequence, although it cannot be assigned to any family based on the top ten sequences. The mFold predicted secondary structure of Tb-1 is shown in Fig. 1B, which has two loops connected by two stem regions.

ThT fluorescence based binding assays

To evaluate the binding property of the aptamers, we first used thioflavin T (ThT) as a fluorescence probe. ThT is most well-known for its ability to bind G-quadruplex structures,[33] but it can also bind to other DNA structures.[27,34] Free ThT is almost non-fluorescent, and its fluorescence increases upon binding to DNA. As a DNA aptamer binds to its target, a fraction of the bound ThT molecules might be released, leading to decreased fluorescence (Fig. 2A).[33] The ThT fluorescence assay has been widely applied to the study of binding to many aptamers.[35,36] To evaluate whether the Tb-1 and Tb-4 aptamers can bind, we titrated Tb^{3+} ions into aptamer/ThT mixtures. The Tb-1 aptamer exhibited over 90% fluorescence drop with a fitted K_d of 106 nM, whereas Tb-4 showed only about 50% fluorescence

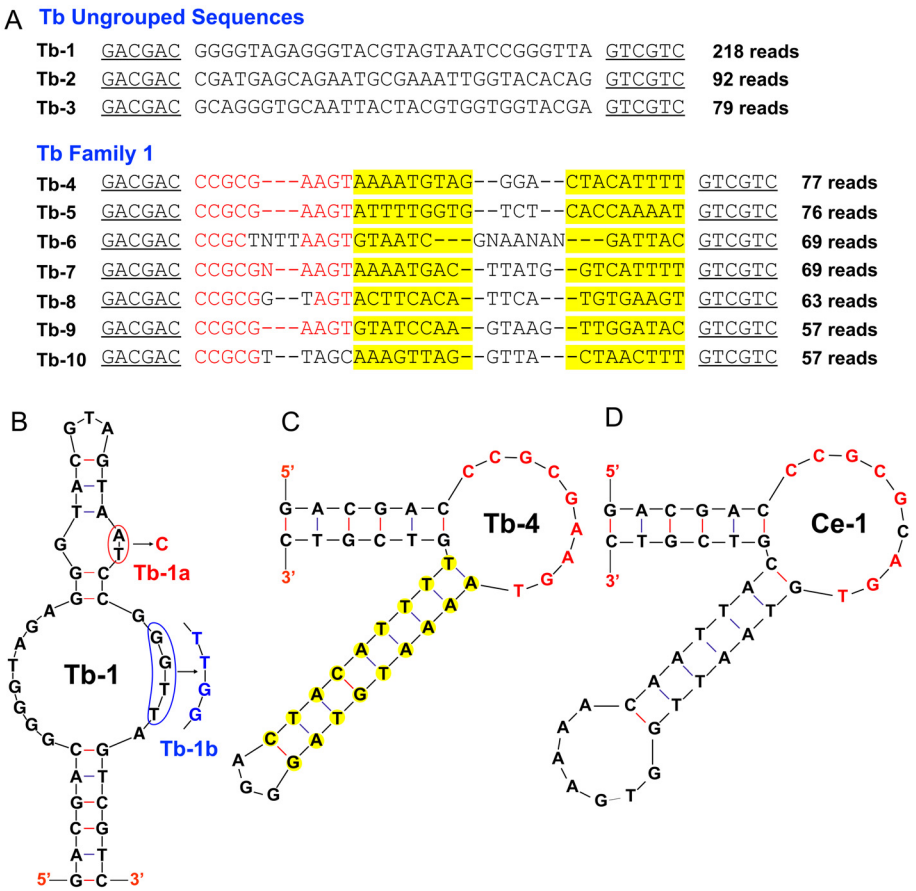

Fig. 1 (A) Alignment of the top 10 sequences from the Tb^{3+} selection. Some ungrouped sequences and one well-aligned family were identified. The nucleotides in the primer-binding regions are underlined, the conserved nucleotides are marked in red, and the yellow highlighted regions can form a stem region in the middle hairpin. The secondary structures predicted by mFold for the (B) Tb-1, (C) Tb-4, and (D) Ce-1 aptamers. Two mutants of Tb-1 are also designed as indicated by the base substitution in red and blue colors.

drop with a K_d of 290 nM (Fig. 2B). The lower K_d indicates that Tb-1 has superior binding for Tb^{3+} compared to Tb-4.

To confirm specific binding, we then performed some mutation studies on Tb-1. First, we mutated the "AT" highlighted by the red circle (Fig. 1B) by a "C" to form a "C–G" pair in the top stem region, and named this mutated aptamer Tb-1a. The ThT fluorescence assay showed that Tb-1a could still bind to Tb^{3+}, whereas the K_d value increased slightly to 244 nM (Fig. 2B). Therefore, we believe that this aptamer has a simple structure with two loops connected by two base paired stems. Furthermore, we replaced the "GGTT" sequence with "TTGG" in the loop region (blue box at position b, Fig. 1B), and named the resulting mutant Tb-1b. This mutant showed significantly weakened binding to Tb^{3+}, and the K_d increased to 1910 nM (Fig. 2B). Nevertheless, 90% fluorescence quenching was still observed upon the addition of 20 μM Tb^{3+}. To test whether such a fluorescence drop was due to nonspecific fluorescence quenching by Tb^{3+}, we tried two unrelated aptamers, OTC43[37] and IBF-1[38] (see Table S1† for their sequences). For these two control aptamers, the fluorescence drop was less than 20% even with 500 μM Tb^{3+} (Fig. S2†). Therefore, Tb-1 and Tb-4 are true aptamers. We then studied the effect of salt and discovered that Mg^{2+} and Na^{+} ions had little effect on the binding property of the Tb-1 aptamer (Fig. S3†).

Tb-1 is selective for lanthanide ions as a group

We then assessed the selectivity of the Tb-1 aptamer. All trivalent rare earth metal ions (excluding radioactive Pm) were tested. Most of these metal ions, except for Sc^{3+}, exhibited a similar degree of fluorescence drop of around 80%, indicating that they can all bind to Tb-1. The fluorescence decrease by Ce^{4+} was insignificant, suggesting this aptamer can only bind to trivalent lanthanides.

Finally, other non-rare-earth metal ions, including Ca^{2+}, Cr^{3+}, Mn^{2+}, Fe^{2+}, Fe^{3+}, Co^{2+}, Ni^{2+}, Cu^{2+}, Zn^{2+}, Cd^{2+}, Ba^{2+}, Hg^{2+}, and Pb^{2+}, were assessed at a higher concentration (5 μM). Among these, Cu^{2+} and Hg^{2+} exhibited a significant fluorescence decrease (purple bars, Fig. 2C) attributable to their strong fluorescence quenching properties. Since Cu^{2+} and Hg^{2+} are strongly thiophilic metals, for analytical applications, 2-mercaptoethanol can be used to chelate them, and this thiol compound should not affect the binding of Tb^{3+}. Indeed, when Cu^{2+} was mixed with 2-mercaptoethanol, no fluorescence decrease was observed. However, upon the addition of Tb^{3+},

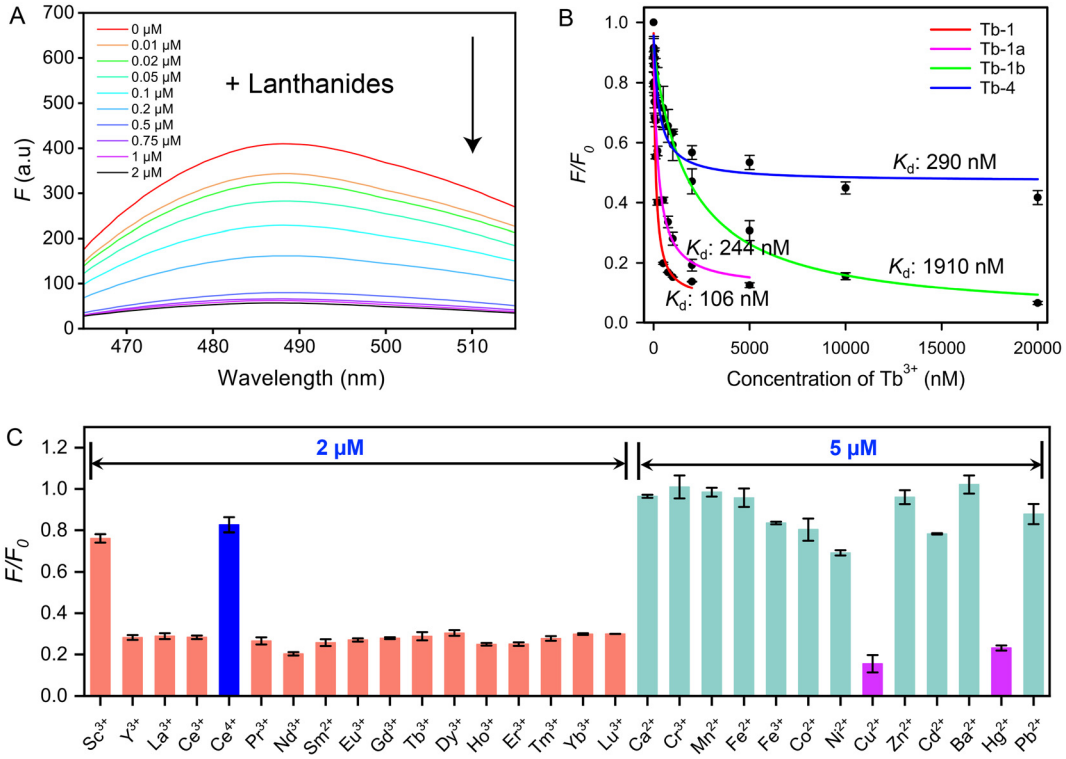

Fig. 2 (A) Fluorescence spectra of titrating Tb^{3+} to a Tb-1/ThT mixture. (B) Titration curves of Tb^{3+} into the Tb-1 aptamer, its two mutations Tb-1a and Tb-1b, and the Tb-4 aptamer. (C) The selectivity of the Tb-1 aptamer against various metal ions using the ThT assay. The reactions were performed with 0.5 μM aptamer, 1 μM ThT in 10 mM MES buffer (pH 6) with 100 mM NaCl and 2 mM $MgCl_2$.

fluorescence quenching occurred again (cyan-blue bars, Fig. S4A†). Similar results were obtained for Hg^{2+} (gray-blue bars, Fig. S4A†). Additionally, a slight fluorescence decrease was observed with Fe^{3+}, Co^{2+}, Ni^{2+}, and Cd^{2+}, which was also attributed to fluorescence quenching as confirmed through a strand-displacement assay (*vide infra*) (Fig. 2C). Therefore, Tb-1 is a general lanthanide binding aptamer.

A light-up DNA strand-displacement biosensor

The ThT fluorescence provides a simple and rapid binding assay, but it is in a signal turn-off mode. Certain metal ions such as Cu^{2+} and Hg^{2+} can strongly quench the fluorescence, leading to false-positive results. A turn-on design can overcome this problem. Therefore, we used a strand-displacement assay, which can also serve as a biosensor. Firstly, the 5′-end of aptamer Tb-1 was labeled with a carboxyfluorescein (FAM) fluorophore (Table S1†). The fluorescence of FAM was quenched upon hybridization with a short quencher-labeled complementary strand. In the presence of a lanthanide ion, binding of the aptamer led to the release of the quencher-labeled strand, resulting in an increase in fluorescence (Fig. 3A).[29,39–41] We used 20 nM FAM-labeled strand and 40 nM quencher labeled strand to achieve a low background. When Tb^{3+} was added, the fluorescence immediately increased, indicating a rapid binding and subsequent release of the quencher-labeled strand. A series of concentrations of Tb^{3+} were tested (Fig. 3B), and a calibration curve with $(F - F_0)/F_0$ was fitted, and an apparent K_d of 72.4 nM was obtained (Fig. 3C). This is not the true K_d of the aptamer due to the presence of the quencher-labeled competing strand. Based on chemical equilibrium, we then calculated the true K_d for Tb-1 to be 3.9 nM, considering the quencher-labeled strand as a competitor (Fig. S6†).[42] Similarly, titration experiments determined the true K_d values for Y^{3+}, La^{3+}, and Lu^{3+} to be 2.7 nM, 26.9 nM, and 2.3 nM, respectively (Fig. S5 and S6†).

The selectivity of aptamer Tb-1 was further tested using the strand-displacement biosensor. Similar to the ThT assay, all rare earth metal ion (0.5 μM each), except for Sc^{3+}, showed a similar fluorescence enhancement. In contrast, Sc^{3+} did not exhibit fluorescence enhancement, suggesting that Tb-1 does not bind to Sc^{3+}, attributable to its much smaller size. Moreover, other metal ions were assessed at higher concentrations (5 μM), and none showed an increase in fluorescence. Notably, Cu^{2+} and Hg^{2+} continued to exhibit fluorescence quenching. Consistent with the ThT assay, 2-mercaptoethanol can mask Cu^{2+} and Hg^{2+} (Fig. S4B†).

Aptamer selection using Ce^{3+} as a target metal ion

So far, Tb^{3+}, Gd^{3+} and Sc^{3+} have been used for aptamer selection. The resulting aptamers either have a similar affinity to all the lanthanide ions or have stronger affinities to heavier ones. Therefore, we wondered whether there are aptamers that can bind to light lanthanides more strongly. So, we chose to use a

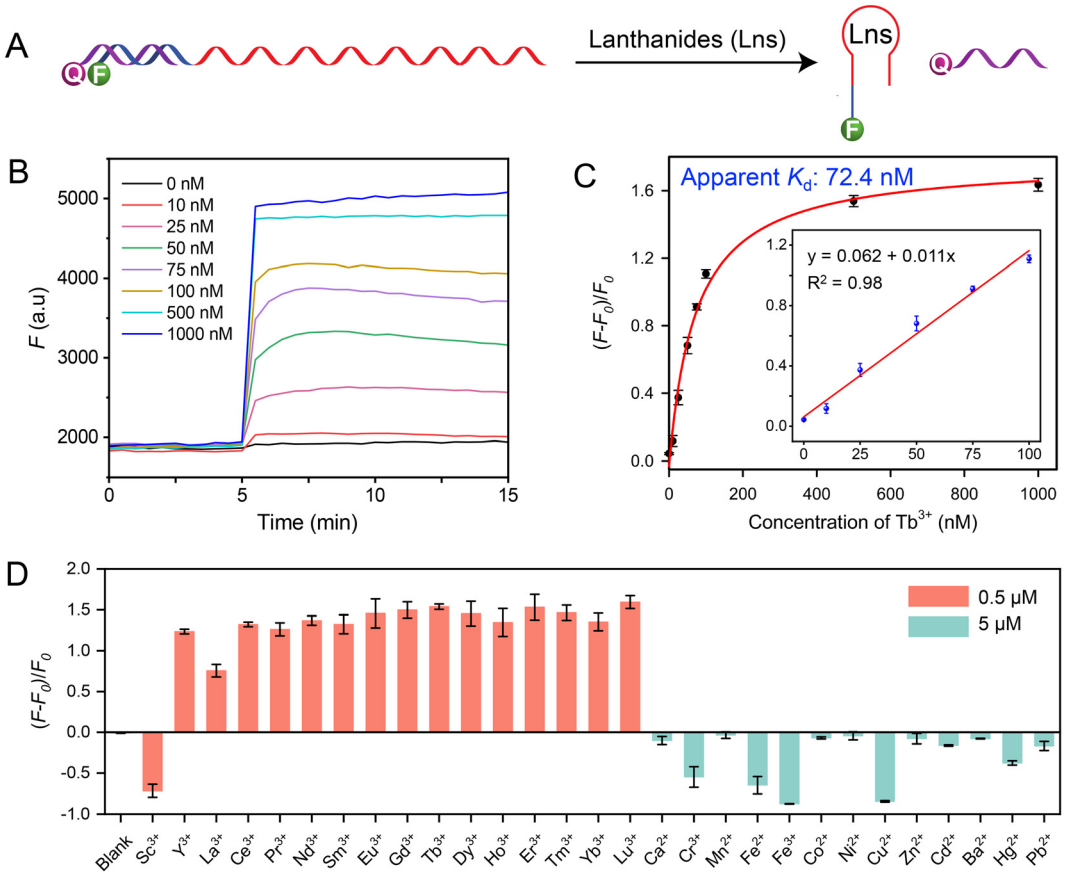

Fig. 3 (A) A scheme of the strand-displacement biosensor featuring a covalently attached fluorophore and quencher. (B) Response of the strand-displacement biosensor to various concentrations of Tb^{3+}. (C) Calibration curves of the biosensor for Tb^{3+}. (D) The selectivity of the Tb-1 strand-displacement biosensor against various metal ions.

light lanthanide, Ce^{3+}, for a new selection. Using 10 μM Ce^{3+} (later reduced to 2 μM), we performed 16 rounds of selection. We aligned the top 20 sequences and found that the top family in the Ce^{3+} selection belonged to family 1 in the Tb^{3+} selection (*e.g.* sequence Ce-1 is very similar to Tb-4, Fig. 1D and Fig. S7A†). Therefore, we did not study this family any further. We picked the first ungroup sequence (Ce-2, Fig. S7B†) for further studies. Using the ThT fluorescence assay, the Ce-2 aptamer showed comparable K_d for Ce^{3+} (169 nM) and Yb^{3+} (343 nM, Fig. S7C†). Thus, it is indeed difficult to find an aptamer that can bind to light lanthanides more strongly. In contrast, the Lu12 DNAzyme reacts faster in the presence of light lanthanide ions.[21] This is an interesting comparison of lanthanides binding by DNAzymes and by aptamers. In DNAzyme catalysis, metal ions only need to serve as a cofactor and they mainly interact with the scissile phosphate group. In aptamers, a stable binding pocket involving nucleobases needs to form. It also needs to be pointed out that a faster DNAzyme cleavage rate does not mean tighter binding.

Comparison of lanthanide binding aptamers: Tb-1, Tb-4, Gd-1 and Sc-1

In this work, we obtained two aptamers: Tb-1 and Tb-4. We then compared them with two previously reported aptamers obtained using Gd^{3+} and Sc^{3+} as target ions. We first used ThT fluorescence to measure the binding of Tb^{3+} by the Gd-1 aptamer and obtained a K_d of 1.5 μM (Fig. 4A). The secondary structure of Gd-1 (Fig. 4A) is quite similar to that of Tb-4. In both aptamers, two base paired stems are right next to each other, and they both contained CCGC in their loop regions. That being said, Tb-4 has a longer conserved loop (mostly purines), which is different from that in the Gd-1 aptamer (mostly pyrimidines). So, the Tb-4 and Gd-1 aptamers are related but different. Overall, the Tb-1 aptamer has higher affinity than both Tb-4 and Gd-1. From the base composition, Tb-1 is rich in guanine in the loops, Tb-4 has a balanced base composition, while Gd-1 is rich in pyrimidines. There are different ways for DNA to bind to lanthanide ions, and guanine-rich aptamers have higher affinities.[43]

Then, we compared Tb-1 with Sc-1. Sc-1 was previously obtained using Sc^{3+} as the target. Unlike Tb-1, Sc-1 binds to Sc^{3+} and exhibits a significant difference in K_d values between light and heavy lanthanide ions, with a K_d of 258.5 nM for La^{3+} and 0.6 nM for Lu^{3+} (a 475-fold difference). In contrast, Tb-1 does not bind Sc^{3+} and shows a much smaller difference in K_d values for light and heavy lanthanide ions, with K_d values of 26.9 nM for La^{3+} and 2.3 nM for Lu^{3+} (a 12-fold difference) (Fig. 4B).

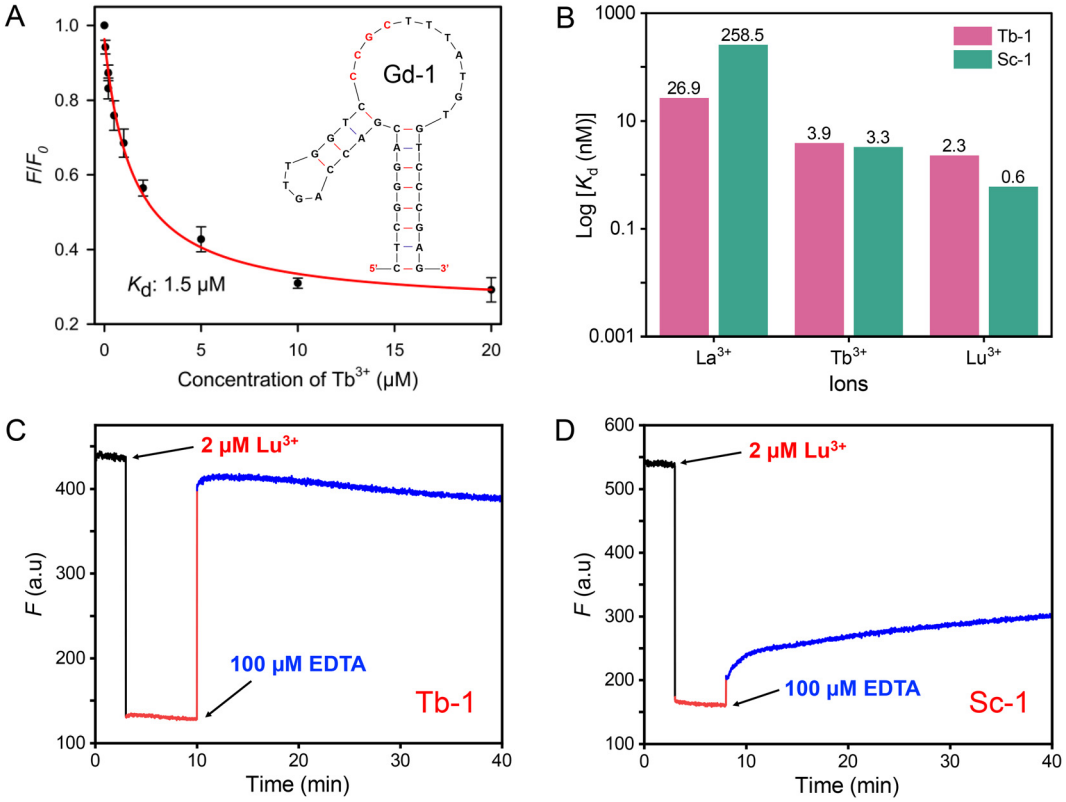

Fig. 4 (A) Titration curves of Tb^{3+} into the previously reported aptamer Gd-1.[28] Inset: predicted secondary structures from mFold. (B) K_d values of the Tb-1 and Sc-1 aptamers for La^{3+}, Tb^{3+}, and Lu^{3+}. Kinetics of fluorescence change of 0.5 μM (C) Tb-1 and (D) Sc-1 aptamer along with 1 μM ThT binding to 2 μM Lu^{3+}, followed by the addition of 100 μM EDTA. Panel (D) adapted from ref. 27 with permission. Copyright 2025 American Chemical Society.

Binding and dissociation kinetics indicating outer-sphere coordination

To gain insights into DNA coordination with lanthanide ions, ligand exchange kinetics is a simple experiment but it can provide key information. For example, inner-sphere coordinated water molecules exchange more slowly with bulk water than outer-sphere coordinated water, which is attributable to the stronger interactions and the need for a more complex mechanism for the inner-sphere exchange.[44] Our previously reported Sc-1 aptamer is featured with slow binding kinetics to heavy lanthanide ions and resistant to dissociation in the presence of EDTA, even though EDTA has over 10 orders of magnitude higher affinity to the lanthanides than Sc-1 has.[29] Such slow binding and dissociation is attributable to an inner-sphere coordination leading to a higher activation energy barrier. To further investigate the binding mechanism of Tb-1 to lanthanide ions, we performed a kinetic assay using ThT fluorescence. After the aptamer/ThT fluorescence stabilized, the addition of 2 μM Lu^{3+} caused a significant fluorescence decrease. Subsequent addition of 100 μM EDTA immediately restored the fluorescence of the Tb-1 sample to its initial level, whereas the Sc-1 fluorescence recovered much more slowly (Fig. 4C and D). Here, we used EDTA to exchange the aptamers for Lu^{3+} binding. This experiment suggests that Tb-1 binds lanthanides *via* outer-sphere interactions, while Sc-1 engages in inner-sphere binding. Further structural biology experiments and advanced spectroscopy studies are needed to confirm this hypothesis.

Regardless of the aptamers, they all showed tighter binding to heavier lanthanide ions. The hydrated ionic radius of lanthanides decreases gradually from 1.16–1.22 Å for La^{3+} to 0.97–1.00 Å for Lu^{3+}.[45,46] This decrease size leads to a higher charge density for heavier lanthanides and thus stronger binding interactions with the aptamers.

Detection of lanthanide ions

In this work, we have obtained an interesting aptamer, Tb-1, which has a high binding affinity to all the lanthanides. To evaluate the analytical performance of the Tb-1 aptamer, we further challenged our strand-displacement biosensor with Lake Ontario water samples. To remove potential interference from unknown substances in lake water, we filtered the samples by using a 0.2 μm membrane. Different concentrations of Tb^{3+} were then added to the filtered water, and each concentration was tested three times. As shown in Fig. 5A, higher Tb^{3+} concentrations resulted in a stronger final fluorescence. We then plotted the final fluorescence as a function of the Tb^{3+} concentration (Fig. 5B). The results demonstrated

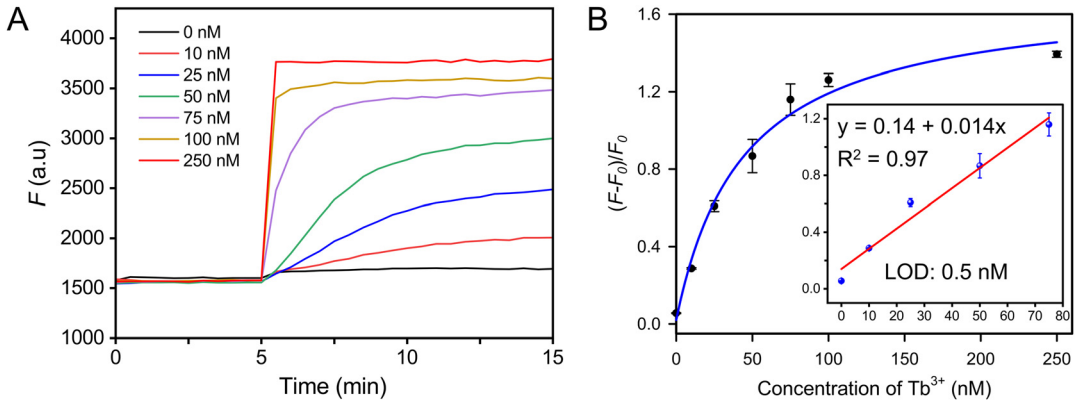

Fig. 5 Fluorescent strand-displacement aptamer biosensor for the detection of Tb^{3+} in Lake Ontario water. (A) Kinetics traces of the 20 nM biosensor in the presence of various concentrations of Tb^{3+} in lake water. (B) The calibration curve of the sensor. Inset: linear response at low Tb^{3+} concentrations. The water contained 10 mM MES, 100 mM NaCl, and 2 mM $MgCl_2$, with the pH adjusted to 6.

that the sensor developed based on aptamer Tb-1 enabled stable and highly sensitive detection of Tb^{3+} in lake waters, with a LOD of 0.5 nM (inset of Fig. 5B). Therefore, this sensor held significant potential for the detection of lanthanide ions.

Conclusions

In this work, we used Tb^{3+} and Ce^{3+} as target metal ions for aptamer selection, and obtained a new high affinity aptamer named Tb-1 that has 3.9 nM K_d for Tb^{3+}. It has slightly higher binding affinity for heavier lanthanides and the K_d difference between La^{3+} and Lu^{3+} is within 12-fold, which can be explained by the size difference of the lanthanides. Upon the addition of EDTA, the fast dissociation of lanthanides from Tb-1 is consistent with an outer-sphere coordination binding model. This is in sharp contrast to the Sc-1 aptamer, which showed a much larger affinity difference for different lanthanides and a very slow EDTA displacement kinetics for Lu^{3+}. We attributed these properties of Sc-1 to inner-sphere binding to heavy lanthanides. Tb-1 is a general lanthanide binding aptamer motif, and we also showed its application for lanthanide detection using a fluorescence DNA strand displacement assay.

Data availability

The data supporting this article have been included as part of the ESI.†

Conflicts of interest

There are no conflicts to declare.

Acknowledgements

This work was funded by the Natural Sciences and Engineering Research Council of Canada (NSERC). Jin Wang, Xin Wang, and Xuesong Li were supported by a China Scholarship Council grant (CSC) for their visit to the University of Waterloo.

References

1 K. Zheng and P. Ma, Recent advances in lanthanide-based POMs for photoluminescent applications, *Dalton Trans.*, 2024, **53**, 3949–3958.
2 P.-J. J. Huang, M. Vazin, J. J. Lin, R. Pautler and J. Liu, Distinction of individual lanthanide ions with a DNAzyme beacon array, *ACS Sens.*, 2016, **1**, 732–738.
3 S. Kobayashi, M. Sugiura, H. Kitagawa and W. W.-L. Lam, Rare-earth metal triflates in organic synthesis, *Chem. Rev.*, 2002, **102**, 2227–2302.
4 F. Wang, Y. Han, C. S. Lim, Y. Lu, J. Wang, J. Xu, H. Chen, C. Zhang, M. Hong and X. Liu, Simultaneous phase and size control of upconversion nanocrystals through lanthanide doping, *Nature*, 2010, **463**, 1061–1065.
5 Q. Yan, C. Liu, X. Zhang, L. Lei and C. Xiao, Selective dissolution and separation of rare earths using guanidine-based deep eutectic solvents, *ACS Sustainable Chem. Eng.*, 2021, **9**, 8507–8514.
6 E. Varbanova and V. Stefanova, A comparative study of inductively coupled plasma optical emission spectrometry and microwave plasma atomic emission spectrometry for the direct determination of lanthanides in water and environmental samples, *Ecol. Saf.*, 2015, **9**, 362–374.
7 M. He, B. Hu, B. Chen and Z. Jiang, Inductively coupled plasma optical emission spectrometry for rare earth elements analysis, *Phys. Sci. Rev.*, 2017, **2**, 20160059.
8 S. K. Pradhan and B. Ambade, Extractive separation of rare earth elements and their determination by inductively

coupled plasma optical emission spectrometry in geological samples, *J. Anal. At. Spectrom.*, 2020, **35**, 1395–1404.
9 N. Khumalo and M. Mathuthu, Determination of trace elements and lanthanide (REE) signatures in uranium mine products in South Africa by means of inductively coupled plasma mass spectrometry, *J. Geochem. Explor.*, 2018, **186**, 235–242.
10 Y. Zhu, K. Nakano, Y. Shikamori and A. Itoh, Direct determination of rare earth elements in natural water samples by inductively coupled plasma tandem quadrupole mass spectrometry with oxygen as the reaction gas for separating spectral interferences, *Spectrochim. Acta, Part B*, 2021, **179**, 106100.
11 P. Das, A. Ghosh and A. Das, Unusual specificity of a receptor for Nd^{3+} among other lanthanide ions for selective colorimetric recognition, *Inorg. Chem.*, 2010, **49**, 6909–6916.
12 F. Zapata, A. Caballero, A. Espinosa, A. Tárraga and P. Molina, A Selective Chromogenic and Fluorescent Molecular Probe for YbIII Based on a Bichromophoric Azadiene, *Eur. J. Inorg. Chem.*, 2010, **5**, 697–703.
13 J. A. Cotruvo Jr, E. R. Featherston, J. A. Mattocks, J. V. Ho and T. N. Laremore, Lanmodulin: a highly selective lanthanide-binding protein from a lanthanide-utilizing bacterium, *J. Am. Chem. Soc.*, 2018, **140**, 15056–15061.
14 W. B. Larrinaga, J. J. Jung, C.-Y. Lin, A. K. Boal and J. A. Cotruvo Jr, Modulating metal-centered dimerization of a lanthanide chaperone protein for separation of light lanthanides, *Proc. Georgian Natl. Acad. Sci.*, 2024, **121**, e2410926121.
15 J. A. Mattocks, J. J. Jung, C.-Y. Lin, Z. Dong, N. H. Yennawar, E. R. Featherston, C. S. Kang-Yun, T. A. Hamilton, D. M. Park and A. K. Boal, Enhanced rare-earth separation with a metal-sensitive lanmodulin dimer, *Nature*, 2023, **618**, 87–93.
16 L. Xu, P. Zhang, Y. Liu, X. Fang, Z. Zhang, Y. Liu, L. Peng and J. Liu, Continuously tunable nucleotide/lanthanide coordination nanoparticles for DNA adsorption and sensing, *ACS Omega*, 2018, **3**, 9043–9051.
17 W. Zhou, R. Saran and J. Liu, Metal sensing by DNA, *Chem. Rev.*, 2017, **117**, 8272–8325.
18 R. Nishiyabu, N. Hashimoto, T. Cho, K. Watanabe, T. Yasunaga, A. Endo, K. Kaneko, T. Niidome, M. Murata and C. Adachi, Nanoparticles of adaptive supramolecular networks self-assembled from nucleotides and lanthanide ions, *J. Am. Chem. Soc.*, 2009, **131**, 2151–2158.
19 P.-J. J. Huang, J. Lin, J. Cao, M. Vazin and J. Liu, Ultrasensitive DNAzyme beacon for lanthanides and metal speciation, *Anal. Chem.*, 2014, **86**, 1816–1821.
20 P.-J. J. Huang, M. Vazin, Ż Matuszek and J. Liu, A new heavy lanthanide-dependent DNAzyme displaying strong metal cooperativity and unrescuable phosphorothioate effect, *Nucleic Acids Res.*, 2015, **43**, 461–469.
21 P.-J. J. Huang, M. Vazin and J. Liu, In vitro selection of a new lanthanide-dependent DNAzyme for ratiometric sensing lanthanides, *Anal. Chem.*, 2014, **86**, 9993–9999.
22 P.-J. J. Huang, M. Vazin and J. Liu, In vitro selection of a DNAzyme cooperatively binding two lanthanide ions for RNA cleavage, *Biochemistry*, 2016, **55**, 2518–2525.
23 V. Dokukin and S. K. Silverman, Lanthanide ions as required cofactors for DNA catalysts, *Chem. Sci.*, 2012, **3**, 1707–1714.
24 H. Yu, O. Alkhamis, J. Canoura, Y. Liu and Y. Xiao, Advances and challenges in small–molecule DNA aptamer isolation, characterization, and sensor development, *Angew. Chem., Int. Ed.*, 2021, **60**, 16800–16823.
25 A. Brown, J. Brill, R. Amini, C. Nurmi and Y. Li, Development of better aptamers: structured library approaches, selection methods, and chemical modifications, *Angew. Chem., Int. Ed.*, 2024, **63**, e202318665.
26 L. Gu, H. Zhang, Y. Ding, Y. Zhang, D. Wang and J. Liu, Capture-SELEX for a short aptamer for label–free detection of salicylic acid, *Smart Mol.*, 2023, **1**, e20230007.
27 K. Yang, N. M. Mitchell, S. Banerjee, Z. Cheng, S. Taylor, A. M. Kostic, I. Wong, S. Sajjath, Y. Zhang and J. Stevens, A functional group–guided approach to aptamers for small molecules, *Science*, 2023, **380**, 942–948.
28 O. Edogun, N. H. Nguyen and M. Halim, Fluorescent single-stranded DNA-based assay for detecting unchelated Gadolinium(III) ions in aqueous solution, *Anal. Bioanal. Chem.*, 2016, **408**, 4121–4131.
29 J. Wang, Y. A. Kaiyum, X. Li, H. Lei, P. E. Johnson and J. Liu, Kinetic and Affinity Profiling Rare Earth Metals Using a DNA Aptamer, *J. Am. Chem. Soc.*, 2025, **147**, 1831–1839.
30 X. Li, Z. Yang, M. Waniss, X. Liu, X. Wang, Z. Xu, H. Lei and J. Liu, Multiplexed SELEX for Sulfonamide Antibiotics Yielding a Group-Specific DNA Aptamer for Biosensors, *Anal. Chem.*, 2023, **95**, 16366–16373.
31 L. Gu, Y. Ding, Y. Zhou, Y. Zhang, D. Wang and J. Liu, Selective Hemin Binding by a Non-G-quadruplex Aptamer with Higher Affinity and Better Peroxidase-like Activity, *Angew. Chem., Int. Ed.*, 2024, **63**, e202314450.
32 L. Gu, Y. Zhang, D. Wang and J. Liu, Light–Up Sensing Citrate Using a Capture–Selected DNA Aptamer, *Adv. Sens. Res.*, 2024, 2300167.
33 F. Y. Khusbu, X. Zhou, H. Chen, C. Ma and K. Wang, Thioflavin T as a fluorescence probe for biosensing applications, *Trends Anal. Chem.*, 2018, **109**, 1–18.
34 Y. Ding, Y. Xie, A. Z. Li, P.-J. J. Huang and J. Liu, Cross-Binding of Four Adenosine/ATP Aptamers to Caffeine, Theophylline, and Other Methylxanthines, *Biochemistry*, 2023, **62**, 2280–2288.
35 J. Wang, Y. Liu, X. Li, H. Lei and J. Liu, A high affinity and selective DNA aptamer for copper ions, *Chem. Commun.*, 2024, **60**, 14272–14275.
36 Y. Liu and J. Liu, Selection of DNA aptamers for sensing uric acid in simulated tears, *Analysis Sensing*, 2022, **2**, e202200010.
37 Y. Zhao, B. Gao, Y. Chen and J. Liu, An aptamer array for discriminating tetracycline antibiotics based on binding-

enhanced intrinsic fluorescence, *Analyst*, 2023, **148**, 1507–1513.

38 J. Wang, X. Li, H. Lei and J. Liu, Selection of DNA aptamers for detecting metronidazole and ibuprofen: two common additives in soft drinks, *Analyst*, 2024, **149**, 5482–5490.

39 R. Nutiu and Y. Li, Structure-switching signaling aptamers, *J. Am. Chem. Soc.*, 2003, **125**, 4771–4778.

40 N. Nakatsuka, K.-A. Yang, J. M. Abendroth, K. M. Cheung, X. Xu, H. Yang, C. Zhao, B. Zhu, Y. S. Rim and Y. Yang, Aptamer–field-effect transistors overcome Debye length limitations for small-molecule sensing, *Science*, 2018, **362**, 319–324.

41 J. Canoura, T. Nguyen, C. Byrd, R. Hill, Y. Liu and Y. Xiao, Generation of High-Affinity Aptamers for Indazole Synthetic Cannabinoids, *Anal. Chem.*, 2024, **96**, 11488–11497.

42 J. Hu and C. J. Easley, A simple and rapid approach for measurement of dissociation constants of DNA aptamers against proteins and small molecules via automated microchip electrophoresis, *Analyst*, 2011, **136**, 3461–3468.

43 Z. Zhang, K. Morishita, W. T. D. Lin, P.-J. J. Huang and J. Liu, Nucleotide coordination with 14 lanthanides studied by isothermal titration calorimetry, *Chin. Chem. Lett.*, 2018, **29**, 151–156.

44 V. Jacques, S. Dumas, W.-C. Sun, J. S. Troughton, M. T. Greenfield and P. Caravan, High-Relaxivity Magnetic Resonance Imaging Contrast Agents Part 2: Optimization of Inner- and Second-Sphere Relaxivity, *Invest. Radiol.*, 2010, **45**, 613–624.

45 P. D'Angelo, A. Zitolo, V. Migliorati, G. Chillemi, M. Duvail, P. Vitorge, S. Abadie and R. Spezia, Revised ionic radii of lanthanoid (III) ions in aqueous solution, *Inorg. Chem.*, 2011, **50**, 4572–4579.

46 V. Solov'ev and A. Varnek, Thermodynamic radii of lanthanide ions derived from metal–ligand complexes stability constants, *J. Inclusion Phenom. Macrocyclic Chem.*, 2020, **98**, 69–78.

